Hindawi
International Transactions on Electrical Energy Systems
Volume 2023, Article ID 9915905, 15 pages
https://doi.org/10.1155/2023/9915905

Research Article

Economic, Technical, and Environmental Benefits of Occupants' Thermal Comfort-Based Heat Loads Participation in Demand Response Program

Mohammadmehdi Sedaghatzadeh,[1] **Mohsen Gitizadeh**,[1] **and Matti Lehtonen**[2]

[1]*Department of Electrical Engineering, Shiraz University of Technology, Shiraz, Iran*
[2]*Department of Electrical Engineering and Automation, Aalto University, Espoo 02150, Finland*

Correspondence should be addressed to Mohsen Gitizadeh; gitizadeh@sutech.ac.ir

Received 23 March 2023; Revised 6 September 2023; Accepted 29 September 2023; Published 13 November 2023

Academic Editor: C. Dhanamjayulu

Copyright © 2023 Mohammadmehdi Sedaghatzadeh et al. This is an open access article distributed under the Creative Commons Attribution License, which permits unrestricted use, distribution, and reproduction in any medium, provided the original work is properly cited.

The electrification of heating and transportation systems is one of the objectives of developed countries to minimize CO_2 emissions. This objective pushes distribution systems' (DBs) operators to incorporate numerous high-power loads into low-voltage networks that were not designed for such loads. DBs' reconfiguration and the loads' flexible characteristics are two remedies exploited to overcome this issue. Heat pumps (HPs), as the most prevalent loads, can be managed by demand response programs (DRPs) to postpone the costly reconfiguration of distribution systems. HPs' DRP participation affects indoor air temperature. If this is not accomplished reasonably, the occupants' thermal comfort (OTC) will be compromised, and it will be impossible to convince them to continue contributing to DRPs. Based on the ASHRAE55 standard and an experimental building electrothermal model, this article presents a novel framework for determining the HPs' DRPs participation. This framework ensures the OTC and optimizes the HPs' DRP participation. The modified IEEE 33-bus network is employed as the test system to evaluate the proposed method. The simulation results confirm the usefulness of the proposed strategy to improve the technical and economic aspects of the network.

1. Introduction

Climate change and its harmful effects forced many countries to sign international agreements to establish a clear direction for the world's energy policy [1]. Increasing the proportion of renewable energy resources is one of the outcomes of these policies. A perfect example is Denmark, where the Danish Energy Agreement in March 2012 [2, 3] considered wind and photovoltaic technologies as the main power resources in the future. Heat and transportation systems should be electrified according to the agreement. Consequently, the number of space conditioning units (SCUs) and plug-in electrical vehicles (PEVs) will increase soon.

These new loads would be both an opportunity and a risk to distribution networks. They are being fed by low-voltage (LV) grids; therefore, a drastic increase in power consumption, congestion, power quality issues, and environmental consequences are probable. On the other hand, DSOs could rely on new load power consumption flexibility to defer power system expansion, tackle new resources' uncertain power generation, and probable operational problems. Changing the time and the amount of energy consumption by new loads, many countries are working to commence or improve the so-called "smart energy system" which facilitates bidirectional communication between all electrified energy sectors. At the same time, they are seeking new technologies which decline new loads' power consumption and mitigate their devastating effects. For instance, China is the world's largest manufacturer and consumer of SCUs and it contributes to nearly a quarter of global space-cooling CO_2 emissions. Chinese recently

argued that by embracing technologies that are constantly optimizing SCUs' power consumption, they will have accumulative CO_2 emissions reductions of 12.8% between 2019 and 2050 and accumulative bill savings of 2620 billion RMB (Chinese currency) for Chinese consumers [4].

One of SCUs' demand response control methods is carried out under the supervision of a central load dispatching center or local control centers. In this method, DSOs with the aid of so-called direct load control (DLC) signals and a communication system regulate SCUs' consumption. Altering SCUs' power consumption will change the indoor air temperature and violate the occupants' thermal comfort (OTC). If the DSO wants to count on SCUs' maximum and consistent participation in DRPs for handling emergencies, the OTC or meeting occupants' real thermal needs should be considered a prerequisite for defining SCUs' degree of flexibility (the main contribution of this paper).

Regarding OTC in SCUs' DRPs participation, authors have embraced three different visions.

1.1. Feedback Based. In this category, the data gathered from an experimental building provide the main foundation of the method. In [5], with the aid of a supervisory control strategy called smart zoning, in each room of the building, set points are regulated so that the whole building's performance from energy consumption and OTC perspectives optimize. In [6], a two-level supervisory closed-loop feedback strategy is exploited. At the first level, each building employs a local closed-loop feedback controller that processes only local measurements; at the upper level, a centralized unit supervises and updates the local controllers intending to optimize the energy cost and thermal comfort. Three occupancy-based SCUs' operational strategies have been utilized in [7] to optimize energy consumption and indoor air quality when a typical variable air volume system serves multiple zones inside a building. Occupancy-based means, based on the length of time residents occupy a specific room and the amount of air entering the area and the consequent temperature are set. In the aforementioned references, OTC is utilized to prove the effectiveness of the proposed methods. However, LV grid's operational objectives, constraints, and parameters are ignored. These methods would not be practical because the main purpose of SCUs' introduction into electrical surveys is their remedial capability in the grid's future operational issues. Moreover, as each occupant would have his own behavior or each room in a building could have a different occupancy pattern, the control algorithm will be so elaborate for the DSO or a load aggregator to adopt for applying to a large number of SCUs.

1.2. Consumer Ideal Temperature Range. In [8], a hierarchical robust distributed optimization is introduced for day-ahead and intraday scheduling operation of flexible devices (electrothermal heating units) within a city district. The paper concentrates on optimization methods. Each consumer introduces a separate objective function to be optimized. In [9], considering self-defined occupant comfort, a mixed-integer linear programming (MILP) approach provides optimal scheduling for electrical loads in a smart building. OTC is used to define the degree of heat pumps' flexibility; however, a consumer can change the degree of flexibility, regardless of weather and network operational status; however, the DSO should define the degree of flexibility to exploit the maximum permanent flexibility of heat pumps. Marco et al. [10] quantifies customer flexibility with an optimization method in which each consumer introduces a desirable temperature and an ideal range for temperature variations. In [11], the loss of dweller-defined thermal comfort and an appropriate payback method are considered for the loss of thermal comfort.

This work shows that the DSO and heat load owners will have fewer economic and technical benefits if the so-called "consumer ideal temperature range" method is adopted.

1.3. OTC Ignorance. In [12], heat pumps are controlled for distribution system overload relief based on local prices; and the OTC is not considered. Heat pumps' thermal settings are altered in [13] based on voltage magnitude and DR signals from the power market; and the effect of heat pump set points alteration on the OTC is not investigated. In [14], an aggregated electrothermal model is described for a group of houses and energy consumption moves in time to balance the grid, and thermal discomfort is permitted. The authors have considered large energy storage capacities to move energy consumption to times when the power generation of renewable energy resources is high. In [15], an algorithm optimizes power peak shaving in a distribution grid while the OTC is maintained based on occupants' definition of thermal comfort. No calculation was carried out to understand if a user's defined thermal comfort is following his real thermal needs. In [16], thermal dynamics of variable speed heat pumps are modeled in detail using a set of piecewise linear equations for two different methods of room temperature control; and the results are contingent upon how an occupant defines his suitable thermal comfort.

In conclusion, different studies investigated the role of controlling HPs, in general words domestic appliances, for low-voltage system management [17–28]. Table 1 compares the papers in which heat pumps are exploited in DRPs.

In this paper, at a given hour, a specific outdoor temperature, and based on the physical characteristics of occupants, the ASHRAE55 standard yields temperature boundaries in which the OTC is satisfied. It is assumed that all inhabitants live in residential complexes with the same dimensions and material features as the Massachusetts Institute of Technology (MIT) experimental building. The electrothermal model of the building determines SCUs' electrical consumption corresponding to the standard-defined temperature boundaries. Finally, the particle swarm optimization algorithm (PSO) determines SCUs' optimal OTC-assured consumptions. Occupants yield all their authority of setting the living place temperature to DSOs, which would be an obstacle to HP's DRPs participation. Therefore, this work assigns proper economic incentives to the owners according to the degree of their DR

Table 1: Comparison of the reviewed papers.

Ref.	Electro-thermal model		Criterion for determining thermal loads flexibility			Considering network operational constraints	Ease of application of the proposed method for a distribution network
	Heat pump	House	Occupants definition	Standard-based	House occupancy pattern		
Baldib et al. [5]							
Korkas et al. [6]							
Anand et al. [7]							
Diekerhof et al. [8]							
Angelis et al. [9]							
Lingxi et al. [11]							
Csetvei et al. [12]							
Mendaza et al. [13]							
Pedersen et al. [14]							
Kim et al. [16]							
Bhattarai et al. [18]							
Arteconi et al. [19]							
Kim et al. [23]							
Tasdighi et al. [27]							
This paper							

participation. Environmental (maximum reduction in CO2 emission) and network infrastructure benefits are highlighted to convince DSOs to adopt the proposed method. This paper defines and contrasts different technical and economic parameters in two scenarios to clarify the necessity of prioritizing OTC in determining the maximum SCUs' DR potential flexibility.

(i) Scenario 1: DSO assigns proper OTC-assured temperature boundaries. DSO, at a given hour, assumes a typical wearing and activity for inhabitants who are living/working in residential complexes with a uniform material and dimension feature. Two cases are pondered in this scenario which will be described in Section 8.

(ii) Scenario 2: the DSO has to maintain house temperature at the dweller's favorite range. As each consumer would have his own definition of his favorite temperature boundary, for more simplification, this work supposes that all consumers define boundaries which are considered to be "warm" for winter and "cold" for summer. Based on the ASHRAE55 standard and typical physical and environmental features of occupants, boundaries are determined to be 18°C–22°C for summer and 25°C–28°C for winter.

The contributions of this paper are listed as follows:

(i) A new vision of thermal load participation in DRPs is defined. The method has its roots in the ASHRAEE55 standard to guarantee the OTC and permanent SCUs' flexibility offered in the power market.

(ii) The electrothermal model of a typical building determines the degree of thermal load flexibility to manage the distribution network problems.

(iii) Consumers have delegated their living place temperature regulation to the DSO and this will deteriorate their ideal comfort. Therefore, this work based on the degree of HP's participation in DRPs contemplates economic covenants between DSO and consumers.

(iv) Congestion improvement is defined as the reduction of the summation of power flows in all lines (the so-called "congestion index"); however, this work proposes a more accurate objective function which maximizes the difference between actual and maximum power flow (capacity release) in every single line.

2. Space Conditioning Units

Thermostatically controlled loads are substantial DRP resources. They will have high penetration and a degree of flexibility. A SCU comprises an evaporator, a compressor, a condenser, and an expansion valve. The heating cycle of a heat pump extracts heat from the air outside, raises its temperature, and heats indoor air with warm air. Liquid refrigerant transforms into a gas by absorbing the outdoor air heat in the evaporator. The compressor raises the gas pressure and temperature. The hot gas passes through a condenser coil in the indoor space. Its temperature is

Table 2: PMV and thermal sensation.

PMV	Thermal indication
+3	Too warm
+2	Warm
+1	A little warm
0	Neutral
−1	A little cold
−2	Cold
−3	Too cold

higher than the indoor air temperature. Therefore, the gas transfers heat to the indoor space and condenses into a liquid. Eventually, the fluid passes through the expansion valve. The cycle terminates by lowering the liquid's pressure and temperature. An air conditioning thermostat is used to control the indoor temperature and is used to adjust the operating time constant of the air conditioning equipment to ensure that the indoor temperature remains within a given range. In winter, when the indoor air temperature falls below a predetermined value (E_C), the compressor turns on and heats the indoor air temperature (T_e_air) to a predefined value ($\overline{E}_C$) and turns off. The same procedure cools the indoor air temperature in summer. The dead band is an important parameter to consider in a thermostat. In DRPs and emergencies such as congestion, the DSO could alter the dead band or SCUs consumption. The ASHRAE55 standard is used to determine $E_C, \overline{E}_C$ so that the OTC is guaranteed while SCUs' consumption decreases.

3. Electrothermal Model for Residential Consumers

Two primary points need to be clarified. First, how much thermal energy is required to create a specific temperature in a building? Second, the SCUs' power consumption corresponding to the temperature should be determined [16, 29] to show how an electrothermal model for a house is built based on its material arrangement and would be used to calculate the electrical consumption of a SCU for setting the indoor air temperature at a predefined value. Each surface in a building could comprise different insulation layers. For each layer, an electrothermal model is exploited for simulation purposes (Figure 1). Two "lumped" thermal resistances (R_{ins} and R_{out}) and one thermal capacity (C_{total}) are the components of the model. R_{ins} and R_{out} are equivalent inside and outside thermal resistances and C_{total} is the total thermal capacity of the layer.

With the help of this basic electrothermal model, a dynamic model for the test room is created. In the model, the heat power injected by the HP (Q_{hp}) maintains the air temperature at a specified value.

Figure 2 shows the schematic of the experimental building room built at MIT; the room has two parts: the climate room and the test room. The climate room temperature variations simulate outdoor temperature variations. The test room has a thermally activated building system (TABS). TABS' ventilation system consists of hot and cold water pipes passing through the floor. The walls have layers of thermal insulation and concrete. Each layer is defined by its thickness, thermal conductivity, specific heat capacity, and density. The test room has a heater and lighting; and the heat generated by these sources simulates thermal losses.

To determine the optimal power consumption of the HP, Figure 3(a) is used as the electrothermal model of the experimental room [29]. All houses in the typical LV system are supposed to be similar to the experimental room from interior space and insulation material perspectives. Especially in commercial-residential complexes where all units have the same material and map characteristics, considering a valid electrothermal model for all houses would be rational.

Electrical resistance model's conductive and convective resistances: voltage and current sources model temperature and heat gains, respectively. Q_{hp} is the value of thermal energy injected into the building and $T_{ambient}$ is the ambient air temperature. Convective and conductive thermal resistance values, R_{cd} and R_{cv}, and thermal capacitance C, could be obtained via the following equations:

$$\text{Rcd} = L.(k.A)^{-1}, \tag{1}$$

$$\text{Rcv} = (h.A)^{-1}, \tag{2}$$

$$C = c_{shc}.L.\rho, \tag{3}$$

where L and A are the thickness and area of the room surface, respectively. The ρ and c_{shc} are the density and specific heat capacity of the surface material. Also, k and h are the conductive and convective heat transfer coefficients; indeed, h is supposed to be 5 W/(m^2·K), regardless of the surface characteristics; Rcv represents the convective resistor.

The dynamic behavior of the building model is ignored because of the following reasons:

(i) The approach proposed by this work is to change the building temperature in a range that the stable OTC is achieved. In other words, occupants feel thermal comfort at temperatures between initial and steady-state values, and heat loads only handle network operational issues. Therefore, there is no need to monitor the temperature values between the initial and steady-state response.

(ii) For a winter day, this paper's proposed method restrains the indoor maximum temperature variation between 19°C and 26°C. If the DSO applies a regulating signal to increase the indoor air temperature from 19°C to 26°C (Q_{hp}), Figure 3(b) shows that the variation takes approximately 50 minutes. Consequently, if the DLC signal is applied 1 hour before the schedule (in the form of day-ahead operational planning), the temperature will be set at the target value. The same goes for a summer day.

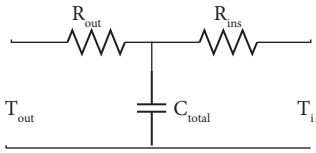

Figure 1: Electrothermal model of a construction element.

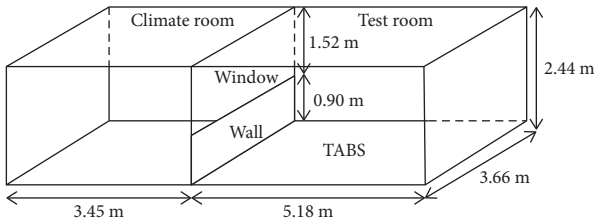

Figure 2: Experimental building room.

4. Thermal Comfort

Thermal comfort is a mental state that expresses the degree of satisfaction of a person from the thermal conditions of the environment. One of the complexities of explaining thermal comfort is that multiple physical parameters are involved.

To achieve the OTC, the following two conditions must be met: (1) the composition of the temperature produced inside the body and the skin temperature must create a neutral thermal sensation (not cold or warm) and (2) the body should have an energy balance, which means that the heat generated by the metabolism is equal to the temperature exchanged between the body and the environment. Relationships between skin and temperature parameters, the degree of heat inside the body, and the amount of physical activity create a neutral sense of warmth in experimental experiments. In these experiments, transpiration rate and skin temperature are measured for different amounts of body metabolism, while the person under the test will have thermal comfort in all conditions. What makes looking into thermal comfort vital is the OTC's great impact on work efficiency. Therefore, the use of SCUs in the DRPs while ignoring the OTC is unacceptable and will lead to a working efficiency decrement.

Predicted mean vote (PMV) is a seven-point scale for heat sensation [30–32]. This index allocates a number for the degree of thermal sensation of individuals. According to an occupant's clothing, metabolism, and physical conditions, the room temperature equals a specified PMV. PMV could be positive or negative. The positive values of Table 2 are equivalent to the temperatures in which the residents feel a little heat, and the negative values of the table correspond to the temperatures that will cause the residents to feel a little cold. The ideal residence's temperature is the one in which occupants feel thermally neutral.

The required formulations for the PMV calculation are provided in [32].

The ASHRAE55 standard in equation (4) introduces an allowable range for PMV deviation from the ideal value. Changing PMV in this range will not disrupt the OTC.

$$-0.5 \le \text{PMV} \le +0.5. \tag{4}$$

5. PMV and Its Impact on the Amount of Thermal Load Participation in DR

This work determines an optimum, day-ahead SCUs' power consumption schedule to manage the congestion in a typical distribution system. For the indoor air temperature, "T_{ideal}" is defined as a temperature at which the PMV is zero. This temperature is the most suitable temperature for occupants. "$T_{\min}$" represents the minimum permissible temperature at which PMV is −0.5 and occupants feel a tolerable sense of coldness. "$T_{\max}$" is the temperature at which PMV is +0.5 and occupants feel a tolerable sense of warmth. Equations that relate indoor air temperatures to PMV are stated in [32].

DSO takes over the authority of occupants to regulate their living place temperature; however, the operator is obliged to bound internal space temperature variations based on these three OTC-assured temperatures. Determining "T_{ideal}," "$T_{\max}$," and "$T_{\min}$" for a specific season and hour in a day, this paper assumes that residents have season-appropriate clothes and activity with a metabolic rate proportional to the hour.

6. OTC-Assured SCUs' Minimum and Maximum Consumption Definition

In summer, if the outdoor temperature goes higher than $T_{\max}$, the minimum power consumption of the thermal load is equal to the power needed for cooling the temperature down to $T_{\max}$, and the maximum consumption of the SCU is the power needed for cooling the temperature down to T_{ideal}. When the temperature is in other areas, the minimum and the maximum consumption of a SCU are as follows:

$$P_{\text{HP}_{\max,\min}} = \begin{cases} \begin{pmatrix} P_{\max} = P_{T_{\min}} \\ P_{\min} = 0 \end{pmatrix}, & T_{\text{ideal}} \le T \le T_{\max}, \\ P_{\max} = P_{\min} = 0, & T \le T_{\text{ideal}}, \end{cases} \tag{5}$$

where $P_{T_{\min}}$ is the power needed to maintain indoor air temperature at $T_{\min}$.

In winter, if the outdoor temperature becomes lower than "$T_{\min}$," then the minimum power consumption of the SCU is equal to the power needed for heating the temperature to $T_{\min}$. Maximum consumption of the load is the power needed for heating the temperature to T_{ideal}. When the temperature is in other areas, the minimum and the maximum consumption of a SCU are as follows:

$$P_{\text{HP}_{\max,\min}} = \begin{cases} \begin{pmatrix} P_{\max} = P_{T_{\min}} \\ P_{\min} = 0 \end{pmatrix}, & T_{\text{ideal}} \le T \le T_{\max}, \\ P_{\max} = P_{\min} = 0, & T \le T_{\text{ideal}}, \end{cases} \tag{6}$$

where $P_{T_{\text{ideal}}}$ is the power needed to maintain indoor air temperature at T_{ideal}.

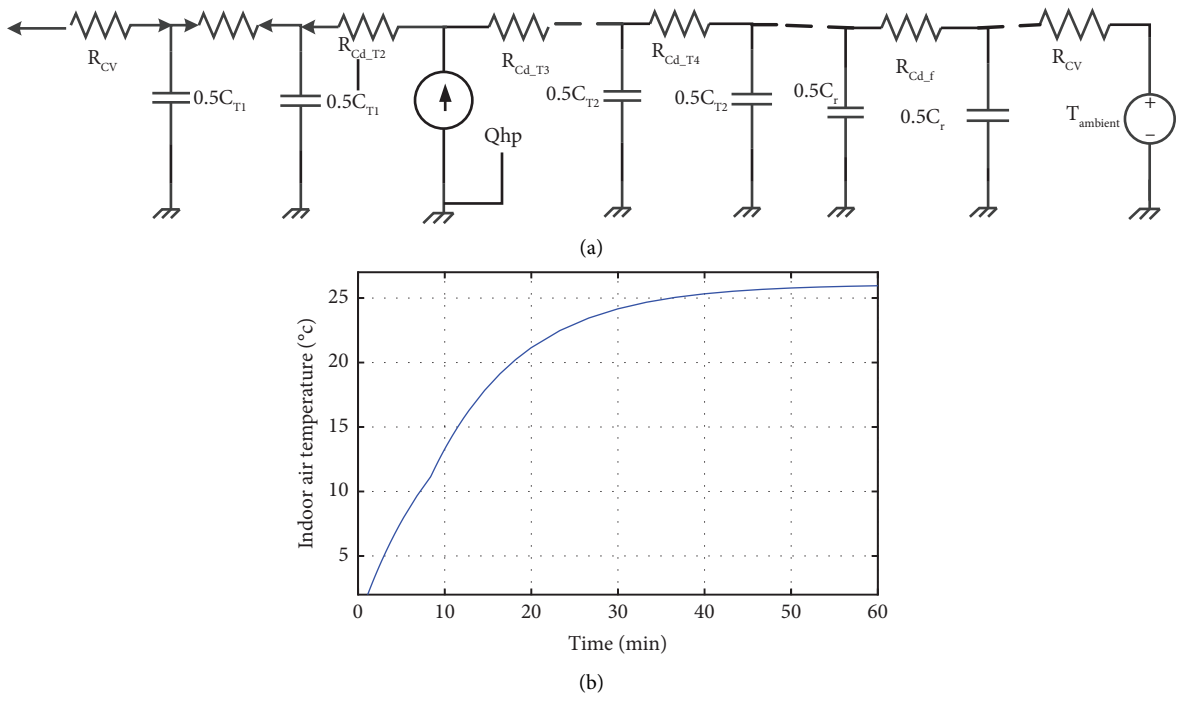

Figure 3: (a) Electrothermal model of the experimental building. (b) Heat time characteristic of the experimental building.

This procedure is simulated using MATLAB software to find an OTC-assured consumption boundary for a given hour, then the boundary is introduced to the PSO, and the optimum consumption for a SCU is determined.

7. Optimization and the Objective Function

7.1. The Standard PSO. The particle swarm optimization algorithm (PSO) is a potent optimization tool in most applications. The optimization problem determines a variable represented by a vector $X = (x_1, x_2, x_3, \ldots, xn)$ that minimizes or maximizes, depending on the proposed optimization formulation and the function $f(X)$. The n-dimension variable vector X is known as the "position vector"; and n represents the number of variables determined in a problem. On the other hand, the function $f(X)$ is called the "fitness function" or the "objective function," which is a function that assesses how good or bad a specific position "X" is.

PSO in each iteration generates a swarm of P position vectors $(X_{ti} = (x_{i1}, x_{i2}, x_{i3} \ldots x_{in})^T)$. The velocity vector $V_{ti} = (v_{i1}, v_{i2}, v_{i3}, \ldots, v_{in})^T$ is calculated to move the position vector from one iteration to the other (7). These two vectors are updated through the dimension j according to the following equations:

$$X_{ij}^{t+1} = X_{ij}^{t} + V_{ij}^{t+1}, \tag{7}$$

$$V_{ij}^{t+1} = wV_{ij}^{t} + \alpha_1 r_1^t \left(p\text{best}_{ij} - X_{ij}^{t}\right) + \alpha_2 r_2^t \left(g\text{best}_{j} - X_{ij}^{t}\right), \tag{8}$$

where $i = 1, 2, \ldots, P$ and $j = 1, 2, \ldots, n$.

At iteration t, three terms determine the velocity vector for the next iteration. $p\text{best}_{ij}$ is a particle's best-achieved value. $g\text{best}_{j}$ is the best point achieved regardless of which particle had found it. The first term in equation (8) is a product between parameter "w" known as inertia weight constant and the particle's previous velocity, which denotes a particle's previous motion into the current one. The individual cognition term, that is, the second term of equation (8), is calculated by using the difference between the $p\text{best}_{ij}$ and the particle's current position X_{ij}^t. As the particle gets farther from the $p\text{best}_{ij}$ position, the difference $p\text{best}_{ij} - X_{ij}^t$ increases and the particle remains close to its best own position. Finally, the third term is social learning and acts as an attraction for the particles to the best point until found at iteration t. Equation (7) updates the particle's positions. α_1, α_2, r_1, and r_2 are coefficients. Koohi et al. [33] elaborate the PSO procedure.

7.2. The Developed Adaptive Particularly Tuneable Fuzzy PSO Algorithm. Particle swarm optimization (PSO) is a metaheuristic optimization technique that solves challenging optimization problems with high efficiency and simplicity. However, several PSO variations exist because the performance of the normal PSO is prone to be caught in local extrema. Fuzzy logic concepts have widely improved the PSO algorithm. In this study, the performance of a modified version of the PSO algorithm known as adaptive particularly tunable fuzzy particle swarm optimization (APT-FPSO) is compared with the performance of the standard PSO. The standard PSO compares the outputs of this work's presented scenarios. Section 8.1 demonstrates that APT-FPSO

produces more acceptable results than the standard PSO. In [34, 35], the APT-PSO optimization method is introduced.

7.3. The Objective Function. The objective function is considered in equation (9).

$$\mathrm{OF} = \sum_{i=1}^{32}\left(\frac{S_{L\_\mathrm{hr}}(l_i)}{S_{L\_\mathrm{hr}\_\max}(l_i)}\right) + \frac{P_{\mathrm{loss-optimized\_hr}}}{P_{\mathrm{loss-nonoptimized\_hr}}} + G, \quad (9)$$

$$g_1 = \sum_{j=1}^{n} \max\left(0, 0.9 - V_{\mathrm{bus}j}\right), \quad (10)$$

$$g_1 = \sum_{j=1}^{n} \max\left(0, V_{\mathrm{bus}j} - 1.1\right), \quad (11)$$

$$G = g_1 + g_2, \quad (12)$$

where $P_{\mathrm{loss-optimized\_hr}}$ is the sum of losses in all lines when SCUs' consumption is optimized. $P_{\mathrm{loss-nonoptimized\_hr}}$ is the sum of losses in all lines when SCUs' consumptions are not optimized. $S_{l\_hr}(l_i)$ is the power flow in line *i*. $S_{l\_hr\_\max}(l_i)$ is the DSO-defined maximum power flow in line *i*. G is a voltage constraint that limits the values between 0.9 and 1.1 (per unit). In the optimization problem, decision variables are power consumptions at each bus (33 decision variables). Some authors used the summation of power flows in all lines as a "congestion index" (objective function) [36]. Minimization of this objective function does not necessarily mean that power flow in every single line is minimized; however, this paper proposes an objective function that is more accurate because it maximizes the difference between actual and maximum power flow in each line. In other words, defining "capacity release" as the objective function will definitely decrease power flows in all lines. G is a penalty factor that restricts all buses' voltages between 0.9 pu and 1.1 pu (equations (10)–(12)).

Figure 4 depicts how the PSO algorithm determines HPs' OTC-based consumption.

8. Results and Discussions

This section introduces several technical, economic, and environmental parameters to justify the effectiveness of the proposed method. Two scenarios are introduced.

Scenario 1 (This Paper's Proposed Method). The DSO assigned a suitable hourly-defined thermal boundary for each group of HPs in the same area. For more simplification, it is supposed that all occupants have season-typical clothes and hour-based metabolic rate. For this scenario, the following two cases are compared:

(i) Without DR (DR = 0), in which all SCUs set house temperatures at T_{ideal} (DR = 0 case)

(ii) Optimized power consumption (OPC), in which DLC signal sets temperatures according to PSO results (OPC case)

Scenario 2 (Old Method ([9, 16]). Occupants intrinsically introduce temperatures that create warm/cold thermal sensations in winter/summer. Therefore, according to Table 2, it is supposed that each consumer group's houses should be cooled down/heated up to temperatures corresponding to PMV = −2 and PMV = +2, respectively. All investigations are carried out for the modified IEEE 33-bus distribution system.

8.1. Optimal Power Consumption Using APT-FPSO and the Standard PSO. Figure 5 compares the HPs' power consumption using the two optimization methods. The APT-FPSO algorithm has reduced the consumption in all buses, and the total amount of consumption reduction is 200 kilowatts, which is equivalent to the typical consumption in bus no. 33 of the IEEE 33-bus network.

Although the APT-FPSO algorithm reduces the optimal consumption of HPs, the amount of this reduction is small in each bus and this point proves the validity of the optimization results using the standard PSO algorithm. Consequently, the simulations required to prove the technical and economic superiority of the scenario proposed in this paper (scenario 1) over the old scenario (scenario 2) will be performed with the standard PSO algorithm.

8.2. Technical Benefits of SCUs' Optimized Consumption. Optimal load flexibility, power flow, congestion index, loss improvement, transformer loss of life, and voltage improvement, as technical parameters, could be utilized as elaborate, technical comparisons between different methods.

8.2.1. Optimal Load Flexibility and Power Consumption Improvement. For scenario 1, Figure 6 depicts the reduction of SCU consumption by employing the scenario. The following equation is used to calculate the optimal load flexibility:

$$P_{L,\mathrm{opt}} = \left(1 - \varepsilon_{\mathrm{optimal}}\right)P_{L,\mathrm{non}}, \quad (13)$$

where $P_{L,\mathrm{opt}}$ and $P_{L,\mathrm{non}}$ are optimized and nonoptimized consumption of HPs in each bus, respectively. $\varepsilon_{\mathrm{optimal}}$ is the optimal flexibility offered by SCUs in DRPs. In each bus, 20% of the load is supposed to be SCUs. In other words, the maximum flexibility available in each bus is 20%. The maximum flexibility defined by the PSO is 7.7% (Figure 7). HPs seem to have a low participation rate (7.7% vs. 20% available). However, the OTC and the consistency of SCU participation are guaranteed. Any other level of HPs' flexibility may violate the OTC. Figure 8 shows the optimal flexibility of heat pumps as a result of applying scenario 2. Scenario 1 increases HPs' optimal flexibility. This superiority is clear when comparing Figures 7 and 8.

8.2.2. Comparison of the Outputs of Two Scenarios. The two proposed scenarios determine different optimized load profiles in each bus. Figure 9 clarifies the differences

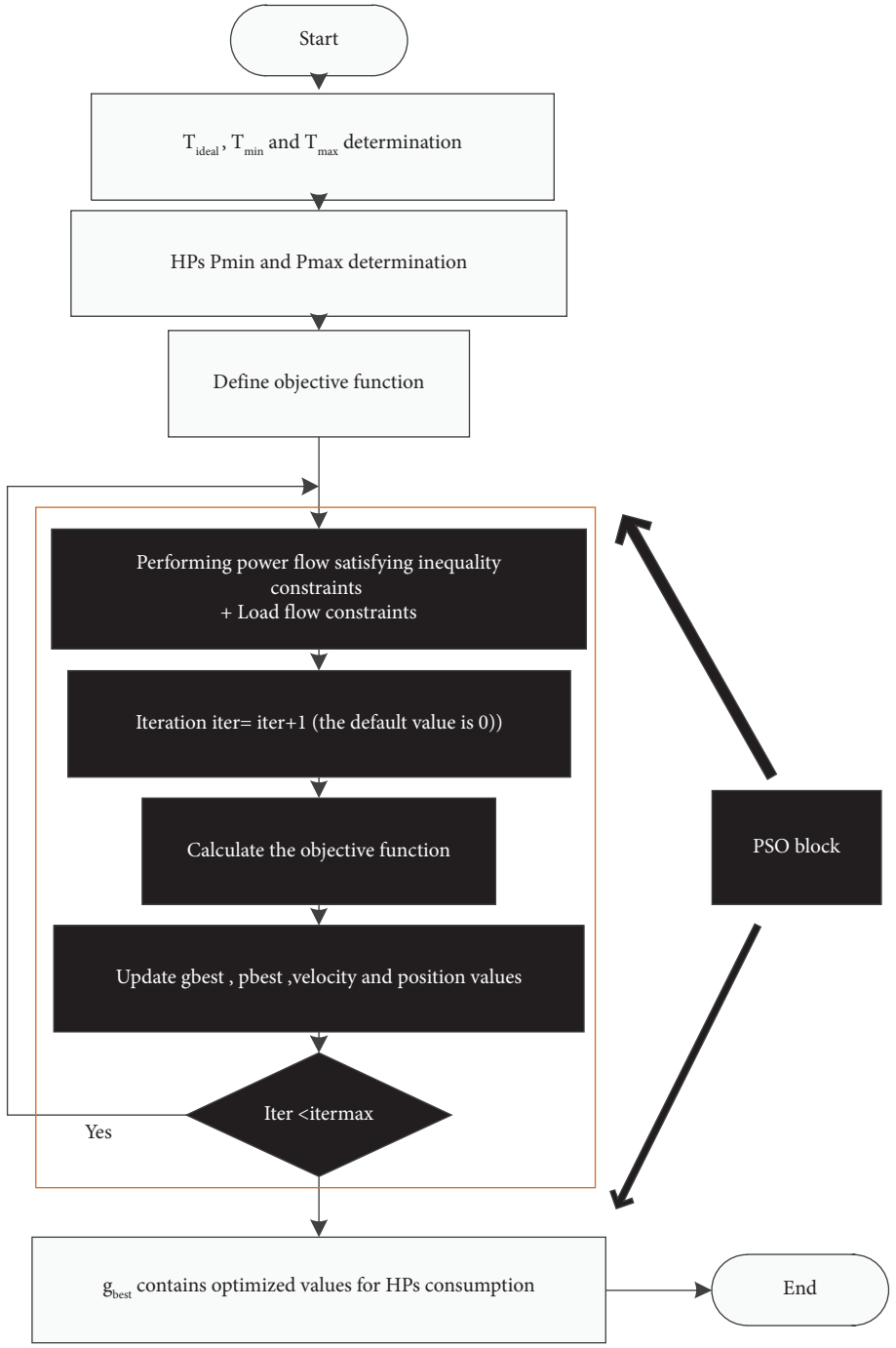

Figure 4: This paper's proposed method.

between the two scenarios' results. Scenario 1, as a substitute for the commonly applied scenario 2, improves the peak shaving on a typical winter day (peak hours occur at midnight when numerous SCUs are on the service to heat buildings).

8.2.3. Power Flow and Congestion Index. The congestion index (CI) for line L is formulated by using the following equation:

$$\mathrm{CI}_L = \sum_{m=1}^{12} S_{L,m}, \tag{14}$$

where $S_{L,m}$ is line L average apparent power flow in the month m. CI is the summation of lines' power flow for a time period t:

$$\mathrm{CI}_t = \sum_{l=1}^{32} S_{L,t}. \tag{15}$$

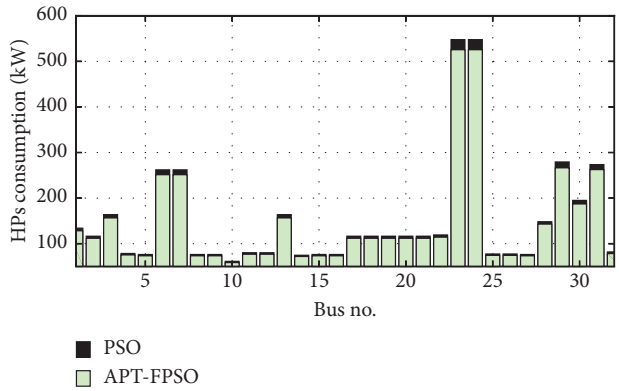

Figure 5: PSO and APT-FPSO optimal HPs consumption.

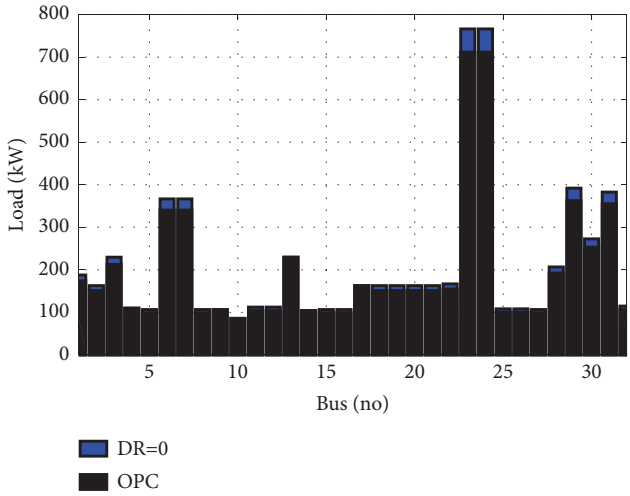

Figure 6: Scenario 1' power consumption improvement.

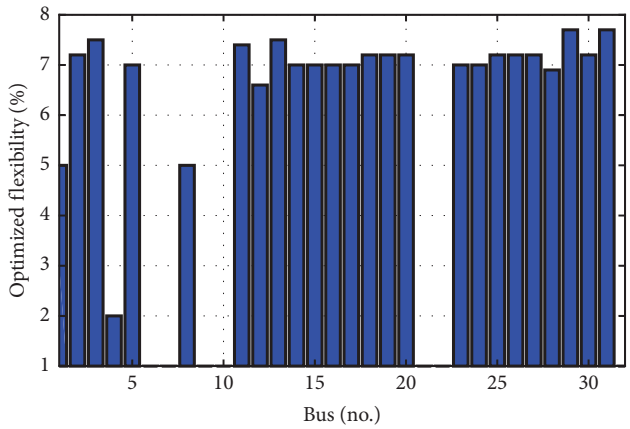

Figure 7: Scenario 1' optimal flexibility.

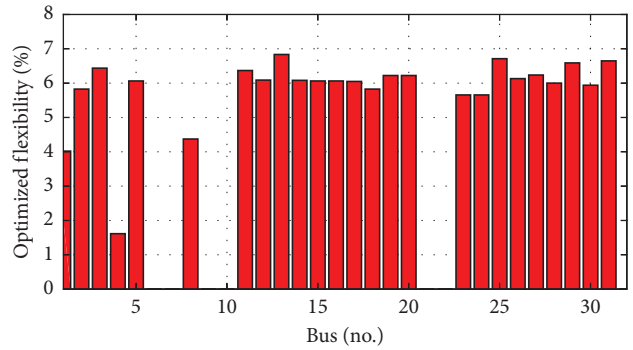

Figure 8: Scenario 2' optimal flexibility.

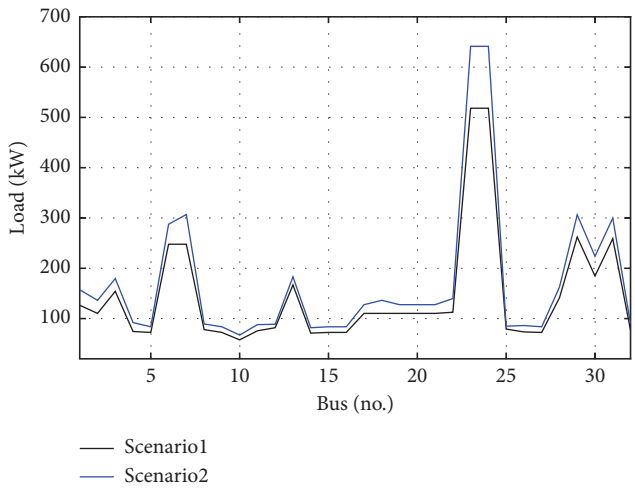

Figure 9: Scenarios' power consumption comparison.

In winter, the peak consumption occurs from 9 PM to 9 AM because SCUs should produce thermal energy to warm rooms. However, this period for summer is from 12 AM to 6:00 PM. Replacing the DR = 0 case with the OPC reduces the power flow by up to 3% (Figure 10). This improvement is achieved when only 20% of loads in each bus are supposed to be SCUs. In other words, only 20% of the total load in each bus is supposed to be controllable, so a 3% improvement could be an acceptable result.

Loads feed from a distribution transformer and line 1 (the line between bus 1 and 2): Figure 11 depicts a noticeable CI1 (15) reduction in winter when OPC and DR = 0 cases are compared in scenario 1. Especially in winter, CI improvement is vital as thermal loads consume higher power to provide the required thermal energy for heating houses (the dashed line shows the OPC case).

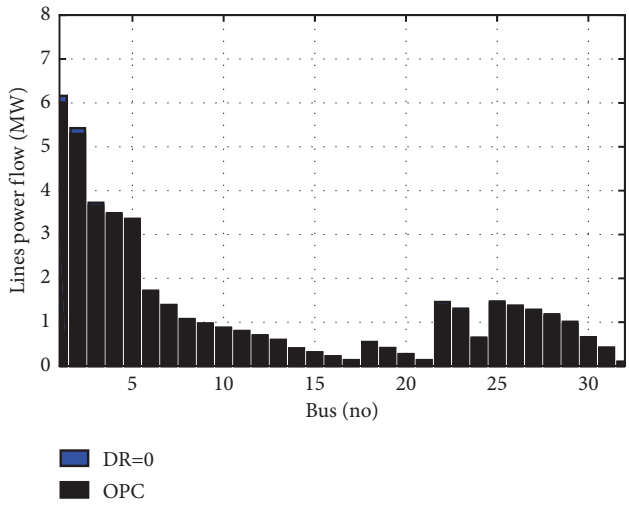

Figure 10: HPs' optimized power consumption impact on lines power flow in scenario 1.

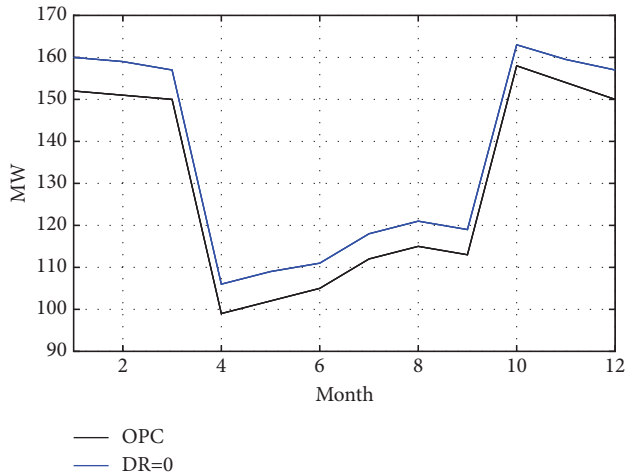

Figure 11: Monthly congestion index in line 1 during a year for scenarios 1 and 2.

8.2.4. Distinction of Two Scenarios. Figure 12 compares the optimized power flows for a winter day peak hour for scenario 1 and scenario 2. The figure depicts 14% power flow reductions in line 1 by choosing scenario 1.

8.2.5. Loss Improvement. Scenario 1 decreases power flows in all lines; consequently, LV grid power losses decrease using this paper's proposed method.

Figure 13 compares total power loss (summation of power losses in all lines) in the network for the same winter day in the OPC and DR = 0 cases. This figure illustrates a maximum 16% reduction in total power loss by applying the first scenario.

8.2.6. Distinction of Two Scenarios. The optimized total power loss on a summer day has a remarkable reduction by utilizing scenario 1 (Figure 14). This fact is more noticeable at peak load hours.

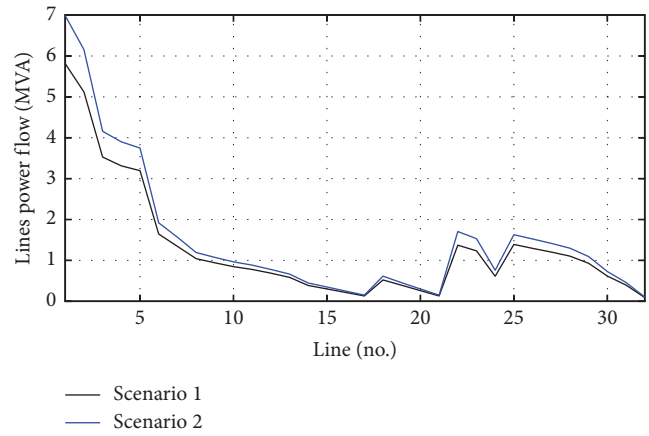

Figure 12: Power flows in a winter day at 24 PM for scenarios 1 and 2.

8.2.7. DS Transformer Loss of Life. The current in line 1 is supposed to be supplied by a 66/20 kV transformer; it is shown that the proposed method affects its hotspot and insulation life.

The heat generated inside a transformer will reduce a specific amount of its life. The aging acceleration factor (FAA in (16)) depicts the dependency of transformer life on its hot spot temperature; indeed, a loss of life index (LOL) determines the reduction of transformer insulation life (equations (16)–(18)).

$$\mathrm{FAA} = e^{\left[(15000/\theta_H 273)-(15000/383)\right]}, \tag{16}$$

where θ_H is the so-called hot spot temperature in ˚C. The equivalent aging factor (FEQA) at the reference temperature in a given time calculates the loss of life.

$$F_{\mathrm{EQA}} = \frac{\sum_{n=1}^{N} (\mathrm{FAA})_n \Delta t_n}{\sum_{n=1}^{N} \Delta t_n}, \tag{17}$$

where Δt_n is the time interval, N is the total number of time intervals, and n is the index of the time interval. For every period, FAA is determined and forms a matrix used by equation (17).

It is necessary to determine the transformer's normal insulation life to determine the percentage of the loss of life equation (18). This model considers 180000 hours or 20.55 years as the normal insulation life.

$$\mathrm{LOL}(\%) = \frac{F_{\mathrm{EQA}} \times t \times 100}{\mathrm{Normal\ insulation\ life}\ (18000)}. \tag{18}$$

In the first scenario for the case DR = 0, LOL for the DB transformer will be 0.7525% which means the transformer loses 1354.5 hours of its life in a year; however, this value is 0.6447% in the OPC case, and the equipment loses 1160 hours of its life in a year. These values show that SCUs' DR participation by utilizing the proposed method adds 195 hours (about 8 days) to the transformer life in a year and about 160 days in its overall life.

8.2.8. Voltage Improvement. As a result of adding new loads to the DBs (increasing power flow in power lines), the magnitude of bus voltages would violate the permissible

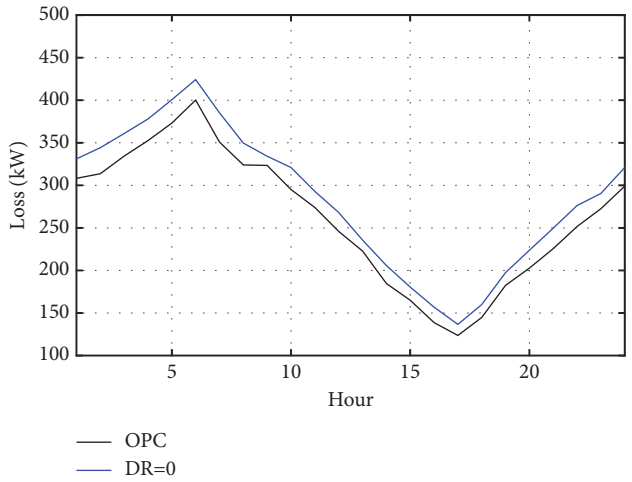

Figure 13: Power loss improvement in a winter day.

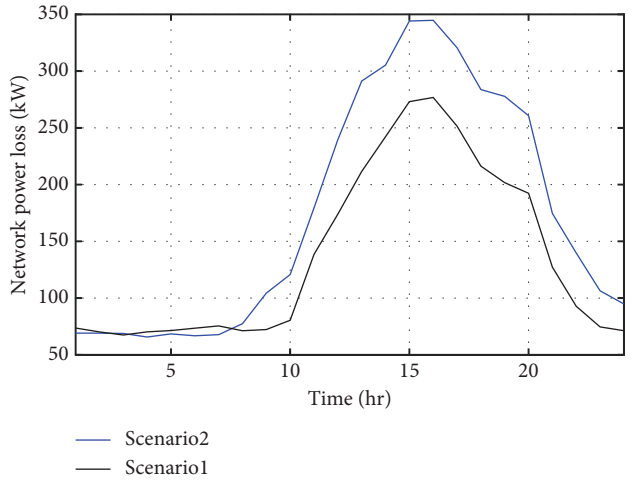

Figure 14: Scenarios optimized power loss parameter in a summer day.

voltage range. In this paper, voltage magnitudes are limited between 0.9 pu and 1.1 pu. Figure 15 compares exploiting the OPC method in scenario 1 in approaching/rising 24-hour voltage magnitudes of bus33 in IEEE 33-bus distribution system to lower limit (0.9 pu), especially at peak hours on a winter day. The OPC corrects the voltage magnitudes between 12 PM and 2 AM (peak hours) and 8 AM to 10 AM.

8.2.9. Distinction of Two Scenarios. Figure 16 compares voltage enhancement between two scenarios. This figure depicts the 24-hour voltage magnitudes of bus 33 because the maximum voltage drop occurs at the end of a radial feeder. For scenario 2, only in the period between 2 PM and 8 PM voltage magnitude is higher than 0.9 pu, whereas, in scenario 1, the voltage magnitude at 7 hours out of 12 peak hours is limited to the permissible boundary. In the remaining 5 hours (3 AM to 8 AM), the voltage magnitude is lower than 0.9 pu, though closer to the limit (0.9 pu) than scenario 2.

For scenario 2, only in the period between 2 PM and 8 PM voltage magnitude is higher than 0.9 pu, whereas, in scenario 1, the voltage magnitude at 7 hours out of 12 peak hours is limited to the permissible boundary. In the remaining 5 hours (3 AM to 8 AM), the voltage magnitude is lower than 0.9 pu, though closer to the limit (0.9 pu) than scenario 2.

8.3. Economic Benefits of SCUs Participation in the DRPs. Two scenarios are applied to a stable LV network in which all operational parameters, including power flows and power losses, are within allowable limits. The two scenarios reduce power flows and power losses; therefore, without causing any operational issues, the difference between power flows and power losses before and after applying the scenarios could be offered by the DSO to a power market. Equation (19) defines "capacity release" as the summation of power flow reduction in the grid. Equation (20) defines the "power loss index" (PLI) as the summation of power loss reduction in the network. The summation of capacity release (CR) and PLI is called "total capacity release (TCR)" and would be traded in a power market (equation (21)). In the following equations, all variables are supposed to be determined at a specific hour, hr.

For reliability purposes, 10% of each line capacity is not considered available.

$$\mathrm{CR_{hr}} = 0.9 \sum_{L=1}^{32} S_{L,\max} - \sum_{L=1}^{32} S_{L,\mathrm{optimal}}, \tag{19}$$

$$\mathrm{PLI_{hr}} = \mathrm{P_{loss-nonoptimized\_hr}} - \mathrm{P_{loss-optimized_{hr}}}, \tag{20}$$

$$\mathrm{TCR_{hr}} = \mathrm{PLI_{hr}} + \mathrm{CR_{hr}}, \tag{21}$$

where $S_{L,\max}$ is the DSO-defined maximum permissible power flow and $S_{l,\mathrm{optimal}}$ is the optimized power at the hour hr.

The DSO can sell TCR according to hourly power tariffs. Power prices are supposed to be the same for low, medium, and peak power periods in summer and winter; however, for the two seasons, they happen at different periods. The annual gross benefit AGB of the DSO could be determined by using the following equation:

$$\mathrm{AGB} = \sum_{hr=1}^{24} \mathrm{tariff_{hr}} \mathrm{TCR_{hr}}, \tag{22}$$

where $\mathrm{tariff_{hr}}$ is the value of the tariff at a specified hour. DSO should consider financial incentives for participants. SCUs will gain benefits in accordance with the level of their participation. A factor, namely, the "thermal load participation factor" (TLPF), is calculated first by using the following equation:

$$\mathrm{TLPF}_{n,\mathrm{hr}} = \left(\frac{P_{L,\mathrm{non}} - P_{L,\mathrm{opt}}}{P_{L,\mathrm{non}}} \right)_{n,\mathrm{hr}} \times 100, \tag{23}$$

$$\mathrm{TLPF_{hr}} = \frac{1}{n} \sum_{n=1}^{32} (\mathrm{TLPF})_{n,\mathrm{hr}}, \tag{24}$$

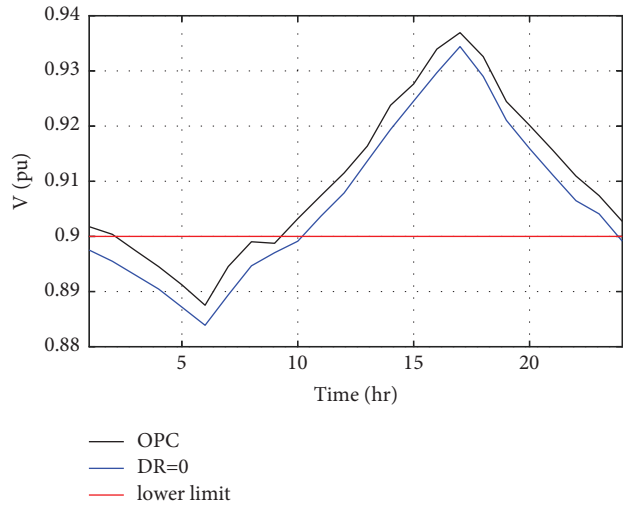

Figure 15: Voltage improvement using scenario 1.

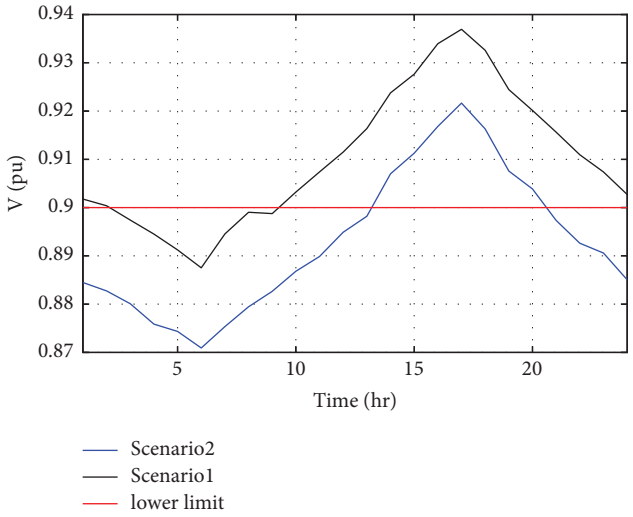

Figure 16: Scenario 1' impact on buses' voltages.

where $P_{L,\text{non}}$ is nonoptimized consumption, $P_{L,\text{opt}}$ is optimized consumption of loads at the hour hr, and n is the bus number.

The nth member of the TLPF vector shows the degree of HPs' contribution on the bus n in the DRPs. TLPF, as the average value of HPs' participation, determines the share of these loads in DRPs (equation (24)).

HPs' incentives (TLI) are assumed to be 30% of the DSO's total. TLI (equation (25)) is higher for the HPS with higher values of the participation factor. Each month's equation (26) determines the pure benefit of the DSO (PDB).

$$\text{TLI}_{\text{hr}} = \begin{cases} 0.05 \times \text{CR}_{\text{hr}}, & 10 \le \text{TLPF}_{\text{hr}} \le 30, \\ 0.1 \times \text{CR}_{\text{hr}}, & 31 \le \text{TLPF}_{\text{hr}} \le 70, \\ 0.15 \times \text{CR}_{\text{hr}}, & 71 \le \text{TLPF}_{\text{hr}}, \end{cases} \tag{25}$$

$$\text{PDB} = \text{AGB} - \sum_{\text{hr}=1}^{24} \text{TLI}_{\text{hr}}. \tag{26}$$

Table 3: Scenario 1 and scenario 2 economic benefits of participation.

Month	TLI_1 ($)	TLI_2 ($)	PDB_1 ($)	PDB_2 ($)
1	793	679	1850	1583
2	803	771	1874	1801
3	798	789	1863	1842
4	239	195	559	456
5	223	192	520	447
6	210	147	490	344
7	169	126	395	294
8	160	132	374	308
9	119	88	278	205
10	775	700	1810	1636
11	816	650	1905	1519
12	832	704	1941	1642

Table 4: Economic benefits surplus of scenario 1.

Month	TESB ($)	DESB ($)
1	114	267
2	32	73
3	9	21
4	44	103
5	31	73
6	63	146
7	43	101
8	28	66
9	31	73
10	75	174
11	166	386
12	128	299

Table 3 is scenario 1's monthly amounts of PDB and TLI parameters.

It is worth reminding that only 20% of HP's penetration has brought the abovementioned benefits. Obviously, with the increment in the number of HPs, which will be inevitable soon, the economic benefits increase for both the DSO and consumers.

Table 4 represents similar data for the second scenario; the table shows the extra money paid to thermal loads and the DSO as the results of scenario 1 exploitation. TESB (thermal loads economic surplus benefit) and DESB (DSO economic surplus benefit) (equations (27) and (28)) prove the economic superiority of the first scenario over scenario 2.

$$\text{TESB} = \text{TLI}_1 - \text{TLI}_2, \tag{27}$$

$$\text{DESB} = \text{PDB}_1 - \text{PDB}_2. \tag{28}$$

Table 4 could be cogent evidence for DSOs and thermal loads to participate in DRPs based on this paper's proposed method. All figures are calculated based on dynamic time-of-use with automation tariff in the UK.

TL1 is scenario 1 and TL2 is scenario 2's thermal loads economic initiative. PDB1 is scenario 1 and PDB2 is scenario 2's pure DSO benefits.

8.4. CO2 Emission. Load consumption optimization contributes to the reduction of CO_2 emissions. This section is about numerically showing and comparing the degree of the two scenarios of environmental preservation. It is supposed that electricity is generated by coal in a power plant. 1 kwh reduction in consumption will lead to a 1000 gr reduction in CO_2 emission [37]. On a typical winter day, the OPC case in the scenario 1 decreases 300 kg of CO_2 emission (in comparison with the DR = 0 case). Indeed, compared with scenario 2, scenario 1 leads to a 400 kg reduction in CO_2 emission in the typical day which is acceptable.

9. Conclusion

This paper is based on the ASHRAE55 standard and represents coincident OTC-assured HPs' participation in DRPs and capacity release maximization in a typical LV system (congestion management). Technical limitations of the LV grid and the electrothermal model of an experimental building are employed. Minimum, ideal, and maximum temperatures of occupants' living places are calculated for one hour. The PSO algorithm determines optimal values for SCUs' consumption and power flows. Different technical and economic parameters motivate HPs' owners and DSOs to apply the proposed scenario. The scenario deprives HPs' owners of the right to regulate the temperature of their houses to maximize the HPs' potential in DRPs. The DSO should be convinced to substitute the proposed method for the one in which each consumer defines its desired temperature range. All the criteria, including technical (optimized HPs power consumption, power flow, network loss, congestion index, DB transformer loss of life, and buses voltage profiles) and economic parameters, demonstrate the superiority of scenario 1 over commonly used scenario 2.

Nomenclature

Acronyms

AGB:	DSO annual gross benefit
CR:	Capacity release
DR:	Demand response
DSO:	Distribution system operator
DLC:	Direct load control
DRPs:	Demand response programs
HPs:	Heat pumps
LV:	Low-voltage grid
MILP:	Mixed-integer linear programming
OTC:	Occupants' thermal comfort
OPC:	Optimal power consumption
PMV:	Predicted mean vote
PEV:	Plug-in electric vehicle
PSO:	Particle swarm optimization algorithm
APT-FPSO:	Tuneable fuzzy particle swarm optimization algorithm
RMB:	Chinese currency
SCU:	Space conditioning unit
TCR:	Total capacity release
TABs:	Thermally activated building systems

Parameters

AGB:	Annual gross benefit ($)
A:	Area of room surface (m^2)
CI_L:	Congestion index for line l
C, C_{total}:	Thermal capacitance ($J{\cdot}K^{-1}{\cdot}kg^{-1}$)
CI_t:	Congestion index for time period t
c_{shc}:	Specific heat capacity (J/kg·K)
DESB:	DSO economic surplus benefit ($)
$\underline{E}_C$:	Cutoff band (°C)
$\overline{E}_C$:	Upper band (°C)
FAA:	Aging acceleration factor
G, g1, g2:	DSO-defined voltage boundaries
G_{best}:	Global best-achieved position
FEQA:	The equivalent aging factor
h:	Convective heat transfer coefficient (W/(m^2·K))
iter:	PSO number of iterations
$iter_{max}$:	Predefined PSO number of iterations
k:	Conductive heat transfer coefficients (m·K/W)
L:	Thickness of the room surface (m)
LOL:	Loss of life (%)
N:	Total number of time intervals
OF:	Objective function
P_{best}:	A particle best-achieved position
PDB:	DSO pure benefit ($)
$P_{HPmin,max}$:	Minimum and maximum consumption of a HP
$P_{T\min}$:	HPs' power consumption proportional to T_{min} (°C)
$P_{loss\_nonoptimized\_hr}$:	Nonoptimized sum of losses (kW)
$P_{loss\_optimized\_hr}$:	Optimized sum of losses (kW)
$P_{L,opt}$:	Optimized consumption of loads (kW)
$P_{T\text{ideal}}$:	HPs' power consumption proportional to T_{ideal} (°C)
P_{max}:	Maximum consumption of a SCU (kW)
P_{min}:	Minimum consumption of a SCU (kW)
PLI:	Power loss index (kW)
$P_{L,non}$:	Nonoptimized consumption of loads (kW)
Q_{hp}:	Heat pump thermal energy (kW)
R_{ins}:	Equivalent inside thermal resistance ($m^2{\cdot}K{\cdot}w^{-1}$)
R_{out}:	Equivalent outside thermal resistance ($m^2{\cdot}K{\cdot}w^{-1}$)
Rcv:	Convective resistance (m^2 K w^{-1})
Rcd:	Conductive resistance ($m^2{\cdot}K{\cdot}w^{-1}$)
$S_{L,max}$:	Maximum permissible power flow in line L (MW)
$S_{L,optimal}$:	Optimal power flow in each line (MW)
$S_{L\text{-hr}}$ (L_i):	Power flow in line i at the hour hr (MW)
$S_{L\text{-hr-max}}$ (L_i):	DSO-defined maximum power flow (MW)
$T_{ambient}$:	Ambient temperature (°C)
TCR:	Total capacity release (MVA)
TLPF:	Thermal loads participation factor ($)
TESB:	Thermal loads economic surplus benefit ($)
TLI1:	Scenario 1's thermal load initiatives ($)

TLI2: Scenario 2's thermal load initiatives ($)
T_{ideal}: PMV is 0 in this ambient temperature (°C)
T_{min}: PMV is −0.5 in this ambient temperature (°C)
T_{max}: PMV is +0.5 in this ambient temperature (°C)
V: Velocity vector
V_{bus}: The magnitude of bus voltage
W: Inertia weight constant
X: Position vector
Θ_H: Transformer hot spot temperature (°C)
Δt_n: Time interval related to FAA
$\mathcal{E}_{optimal}$: Optimized heat load flexibility
α_1, α_2: PSO weight constants
r_1, r_2: PSO weight constants
ρ: Density of the surface materials (kg/m^3).

Data Availability

The data used to support the findings of the study are available from the corresponding author upon request.

Conflicts of Interest

The authors declare that they have no conflicts of interest.

Acknowledgments

The authors thank Shiraz University of Technology for their support. This project was funded by the authors.

References

[1] The Paris agreement, "The first-ever universal, legally binding global climate deal Paris agreement climate conference (COP21)," 2015, https://unfccc.int/process-and-meetings/the-paris-agreement.

[2] The Danish Energy Agreement of Climate, "Accelerating green energy towards 2020. Energy building," 2020, https://ens.dk/sites/ens.dk/files/EnergiKlimapolitik/accelerating_green_energy_towards_2020.pdf.

[3] Denmark, "The intelligent energy system of the future Danish ministry climate, energy build, smart grid strategy," 2013, https://ens.dk/sites/ens.dk/files/Globalcooperation/smart_grid_strategy_eng.pdf.

[4] N. Karali, N. Shah, W. Y. Park et al., "Improving the energy efficiency of room air conditioners in China: costs and benefits," *Applied Energy*, vol. 258, pp. 114023–114112, 2020.

[5] S. Baldi, C. D. Korkas, M. Lv, and E. B. Kosmatopoulos, "Automating occupant-building interaction via smart zoning of thermostatic loads a switched self-tuning approach," *Applied Energy*, vol. 231, pp. 1246–1258, 2018.

[6] C. D. Korkas, S. Baldi, I. Michailidis, and E. B. Kosmatopoulos, "Occupancy-based demand response and thermal comfort optimization in micro grids with renewable energy sources and energy storage," *Applied Energy*, vol. 163, pp. 93–104, 2016.

[7] P. Anand, C. Sekhar, D. Cheong, M. Santamouris, and S. Kondepudi, "Occupancy-based zone-level VAV system control implications on thermal comfort, ventilation, indoor air quality and building energy efficiency," *Energy and Buildings*, vol. 204, pp. 109473–109514, 2019.

[8] M. Diekerhof, F. Peterssen, and A. Monti, "Hierarchical distributed robust optimization for demand Response Services," *IEEE Transactions on Smart Grid*, vol. 9, no. 6, pp. 6018–6029, 2018.

[9] F. De Angelis, M. Boaro, D. Fuselli, S. Squartini, F. Piazza, and Q. Wei, "Optimal home energy management under dynamic electrical and thermal constraints," *IEEE Transactions on Industrial Informatics*, vol. 9, no. 3, pp. 1518–1527, 2013.

[10] P. Marco, J. L. Cremer, F. Ponci, and A. Monti, "Impact of customers flexibility in heat pumps scheduling for demand side management," in *Processings of the IEEE. International Conference on Environment and Electrical Engineering*, pp. 1–6, Milan, Italy, July 2017.

[11] Z. Lingxi, N. Chapman, and N. Good, "Exploiting electric heat pump flexibility for renewable generation matching," in *Processings of the IEEE. International Conference IEEE Manchester Power Technology*, pp. 1–6, Manchester, UK, June 2017.

[12] Z. Csetvei, J. Ostergaard, and P. Nyeng, "Controlling price responsive heat pumps for overload elimination in distribution systems," in *Processings of the 2nd IEEE PES International Conference and exhibition on Innovative Smart Grid Technologies*, pp. 1–8, Manchester, UK, December 2011.

[13] I. D. C. Mendaza, I. G. Szczesny, J. R. Pillai, and B. Bak-Jensen, "Demand response control in low voltage grids for technical and commercial aggregation services," *IEEE Transactions on Smart Grid*, vol. 7, no. 6, pp. 2771–2780, 2016.

[14] T. S. Pedersen, K. M. Nielsen, and P. Andersen, "Maximizing storage flexibility in an aggregated heat pump portfolio," in *Processings of the IEEE Conference on Control Applications*, pp. 1–6, Juan Les Antibes, France, October 2014.

[15] J. Cremer, M. Pau, F. Ponci, and A. Monti, "Optimal scheduling of heat pumps for power peak shaving and customers thermal comfort," in *Processings of the International Conference EEEIC/I&CPS Europe*, pp. 23–34, Palermo, Italy, June 2018.

[16] Y. J. Kim, L. K. Norford, and J. L. Kirtley, "Modeling and analysis of a variable speed heat pump for frequency regulation through direct load control," *IEEE Transactions on Power Systems*, vol. 30, no. 1, pp. 397–408, 2015.

[17] T. Zakula, P. R. Armstrong, and L. Norford, "Modeling environment for model predictive control of buildings," *Energy and Buildings*, vol. 85, pp. 549–559, 2014.

[18] B. P. Bhattarai, B. Bak-Jensen, J. R. Pillai, and M. Mair, "Demand flexibility from residential heat pump," in *Processings of the IEEE PES General Meeting Conference Exposition*, pp. 1–5, National Harbor, MD, USA, July 2014.

[19] A. Arteconi, N. J. Hewitt, and F. Polonara, "Domestic demand-side management (DSM): role of heat pumps and thermal energy storage (TES) systems," *Applied Thermal Engineering*, vol. 51, no. 1-2, pp. 155–165, 2013.

[20] M. Pau, F. Cunsolo, J. Vivan, F. Ponci, and A. Monti, "Optimal scheduling of electric heat pumps combined with thermal storage for power peak shaving," in *Processings of the IEEE International Conference on Environment and Electrical Engineering*, pp. 1–6, Palermo, Italy, June 2018.

[21] C. L. Su and D. Kirschen, "Quantifying the effect of demand response on electricity markets," *IEEE Transactions on Power Systems*, vol. 24, no. 3, pp. 1199–1207, 2009.

[22] A. G. Vlachos and P. N. Biskas, "Demand response in a real-time balancing market clearing with pay-as-bid pricing," *IEEE Transactions on Smart Grid*, vol. 4, no. 4, pp. 1966–1975, 2013.

[23] Y. Kim and L. K. Norford, "Optimal use of thermal energy storage resources in commercial buildings through price-

based demand response considering distribution network operation," *Applied Energy*, vol. 193, pp. 308–324, 2017.

[24] Z. Xu, X. Guan, Q. S. Jia, J. Wu, D. Wang, and S. Chen, "Performance analysis and comparison on energy storage devices for smart building energy management," *IEEE Transactions on Smart Grid*, vol. 3, no. 4, pp. 2136–2147, 2012.

[25] Z. Chen, L. Wu, and Y. Fu, "Real-time price-based demand response management for residential appliances via stochastic optimization and robust optimization," *IEEE Transactions on Smart Grid*, vol. 3, no. 4, pp. 1822–1831, 2012.

[26] P. Du and N. Lu, "Appliance commitment for household load scheduling," *IEEE Transactions on Smart Grid*, vol. 2, no. 2, pp. 411–419, 2011.

[27] M. Tasdighi, H. Ghasemi, and A. Rahimi-Kian, "Residential microgrid scheduling based on smart meters data and temperature dependent thermal load modeling," *IEEE Transactions on Smart Grid*, vol. 5, no. 1, pp. 349–357, 2014.

[28] D. Papadaskalopoulos, G. Strbac, P. Mancarella, M. Aunedi, and V. Stanojevic, "Decentralized participation of flexible demand in electricity markets – Part II: application with electric vehicles and heat pump systems," *IEEE Transactions on Power Systems*, vol. 28, no. 4, pp. 3667–3674, 2013.

[29] T. Zakula, *Model predictive control for energy efficient cooling and dehumidification*, Ph.D. thesis, Massachusetts Institute of Technology, Cambridge, MA, USA, 2013.

[30] ANSI/ASHRAE standard 55-2004, "Thermal environmental conditions for human occupancy," 2004, https://www.ditar.cl/archivos/Normas_ASHRAE/T0080ASHRAE-55-2004-Thermal EnviromCondiHO.pdf.

[31] American Society of Heating Refrigerating and Air-Conditioning Engineers, *2020 ASHRAE handbook—HVAC systems and equipment*, American Society of Heating Refrigerating and Air-Conditioning Engineers Incorporated (ASHRAE), Peachtree Corners, GA, USA, 2020.

[32] ISIRI, *Determination of Thermal Comfort PMV and PPD Indices and Local Thermal Comfort Criteria*, Institute of Standards and Industrial Research of Iran, Tehran, Iran, 1st edition.

[33] I. Koohi and V. Z. Groza, "Optimizing particle swarm optimization algorithm," in *Processings of the IEEE 27th Canadian Conference Electrical and Computer Engineering, (CCECE)*, pp. 1–5, Toronto, Canada, May 2014.

[34] N. Bakhshinezhad, S. A. Mir Mohammad Sadeghi, A. R. Fathi, and H. R. Mohammadi Daniali, "Adaptive particularly tunable fuzzy particle swarm optimization algorithm," *Iranian Journal of Fuzzy Systems*, vol. 17, no. 1, pp. 65–75, 2020.

[35] P. Melin, F. Olivas, O. Castillo, F. Valdez, J. Soria, and M. Valdez, "Optimal design of fuzzy classification systems using PSO with dynamic parameter adaptation through fuzzy logic," *Expert Systems with Applications*, vol. 40, no. 8, pp. 3196–3206, 2013.

[36] C. Murphy, A. Soroudi, and A. Keane, "Information gap decision theory-based congestion and voltage Management in the Presence of uncertain Wind Power," *IEEE Transactions on Sustainable Energy*, vol. 7, no. 2, pp. 841–849, 2016.

[37] L. Wilson, "Electricity emissions around the world," 2020, http://shrinkthatfootprint.com/electricity-emissions-around-the-world.